Sule Lamido University Journal of Science and Technology (SLUJST) Vol. 1 No. 1 [June, 2020], pp. 73-79

Quasiparticle Effects in Bulk and Monolayer of CuSbS2 Band Structure for Solar Cells and Optoelectronic Application

Abdullahi Lawal[1*], L S Taura[2], and M.L. Madugu[3]

[1]Department of Physics, Federal College of Education Zaria, P.M.B 1041, Zaria,Kaduna State
[2]Department of Physics, Sule Lamido University, Kafin Hausa, Jigawa State, Nigeria [3]Department of Physics, Gombe State University, P.M.B. 127, Gombe, Gombe State, Nigeria
*Corresponding Author: abdullahikubau@yahoo.com; lawansani21@gmail.com; maduguu2@gmail.com

Abstract

Copper antimony sulphide ($CuSbS_2$) a layered material is considered as the suitable alternative photovoltaic material with interesting and promising properties along with the abundant, less toxic and economical constituent elements. Therefore, to expose its hidden potentials, detailed knowledge of its structural and electronic properties at the level of reliable and more efficient techniques is very essential. In this study, theoretical calculations of structural and electronic properties of bulk and monolayer of $CuSbS_2$ are presented by highly accurate first-principle approach within many-body perturbation theory (MBPT) based on GW approximation. The calculated structural parameters with inclusion of van der Waals corrections are reasonably close to experimental result. Many-body perturbation theory (MBPT) based on GW approximation (G0W0) were used for quasiparticle (QP) band structure. The bandgap value of 1.4 eV for bulk and 0.64 eV for monolayer calculated with G0W0 are consistence with experimental values. Interestingly, direct band gap nature and narrowing effect of $CuSbS_2$ monolayer suggest that the investigated material is suitable for solar cells and optoelectronic applications.

Key words: *DFT; CuSbS2; Quasiparticle; monolayer; Solar cell.*

1.Introduction

To deal with global energy demand, harvesting solar energy using photovoltaic PV technology is considered amongst the best way, since the resource is renewable with minimal adverse effects on the environment (Al Jibouri & Buckley, 2020). The conversion of light into electricity described through PV effect can be traced back from the liquid electrolytes study by Becquerel's in 1839 (Becquerel, 1839). Rapid development that has steadily improved over years through researchers and industrial laboratories has propelled PV technology into reality. In 1954, Chapin et al. (Chapin, Fuller, & Pearson, 1954) have pioneered a silicon-based p-n junction device with power conversion efficiency of 6%. Since then, sufficiently great momentum is recognized, and domination of crystalline silicon is observed in the PV research area (Sharma & Chandel, 2016). Utilization of silicon-based PV modules remained dominant for decades until energy challenge has been disputed in mankind due to the rise in population and globalization (Zou et al., 2019). Hence, a necessity in finding photoactive materials with better performance, lifetime, abundant availability, cost-effective and environment-friendly are demanded to meet the mankind needs (Javed et al., 2020). Although many absorber materials have been established for solar cell technology, however the achievement of low-cost, non-toxic abundant and efficient solar cell materials are still challenging job for researchers (Pitchaiya et al., 2020). The most significant objectives of the current photovoltaic technology are to acquire a device with lowest industrial cost, low payback time and of higher efficiency. Presently, copper antimony sulphide ($CuSbS_2$) a less-toxic, low-temperature thermoelectric and abundant material could be a better replacement to the toxic, expensive, and scarce materials being used as an absorbing layer for solar cell application (Wan et al., 2019). It can also be used for cooling application devices due to its higher thermoelectric dimensionless figure of merit ZT (Nagaoka et al., 2019). $CuSbS_2$ has the

crystalline orthorhombic layered structure (Pnma; space group 62) as displayed in Figure 1 (Sivagami, Biswas, & Sarma, 2018). The unit cell has a total of 16 atoms including 4 Cu atoms, 4 Sb atoms and 8 S atoms. The lattice parameters of CuSbS2 are $a = 6.045$ Å, $b = 3.807$ Å and $c = 14.545$ Å (Sivagami et al., 2018). There are some advantages of such layered material structure such as structural stability, good charge transport properties and the ability to form interface structure comparing with other structural forms. It was found by the theoretical simulation of defects structure and phase stability using first-principles study that CuSbS2 has p-type conductivity because of the shallow defects of copper vacancy with lowest formation energy in all electrochemical potential conditions (Welch, Zawadzki, Lany, Wolden, & Zakutayev, 2015; Yang et al., 2014). Computationally, ab initio methodologies based on Density Functional Theory (DFT) are intensely used by the theoretical researchers to solve the complex problems (LAWAL, 2017; Lawal, Shaari, Ahmed, & Jarkoni, 2017a; Lawal, Shaari, Ahmed, & Taura, 2018; Lawal et al., 2019). It was found to be more reliable and provides better results regarding electronic structure calculations in designing new materials without prior to experimental knowledge (Lawal, Shaari, Ahmed, & Jarkoni, 2017b, 2017c). This feature of DFT has brought a new insight into the investigation and educational field. In this work, structural parameters calculations of CuSbS2 in bulk and monolayer are performed within the framework of DFT as implemented in Quantum Espresso package (Giannozzi et al., 2009). Electronic properties are calculated using many-body perturbation theory (MBPT) by means of G0W0 approximation as implemented in YAMBO package (Marini, Hogan, Grüning, & Varsano, 2009).

2. Methodology

In this study all calculations have been performed with fully optimized atomic internal coordinates and lattice parameters for full first-principles philosophy. Structural and electronic properties of $CuSbS_2$ are performed within the framework of DFT. Generalized Gradient Approximation (GGA-PBE) formulated by Perdew et al. (Perdew, Burke, & Ernzerhof, 1996)was used. All the calculations are computed via Quantum Espresso and Yambo codes within plane wave pseudopotential approach. The irreducible Brillouin zone (IBZ) was integrated with 10×10×10 k-point sets generated via Monkhorst–Pack approch for self-consisted field calculations (scf) in the case of bulk form of $CuSbS_2$. Norm-conserving pseudopotentials were employed to model the interactions between valence electrons and ionic core. The Kohn-Sham wave functions were expanded with kinetic energy cutoff of 530 eV. The convergence criteria for energy were assumed to be10^{-4}Ry. Full relaxations of $CuSbS_2$ in bulk form were performed to obtain the equilibrium atomic positions and lattice parameters. For monolayer, the calculations were converged with 11×11×1 k-points of the Monkhorst-Pack grid and a vacuum width of 25 Å as can be seen in Figure 2. All forces on each atom were minimized within $0.04\ eV/$Å. Quasiparticle band structure of $CuSbS_2$ were calculated by GW approximation for the self-energy operator Σ. Specifically, frequency dependence of the dielectric matrix were treated by single one shot G_0W_0 approximation via Godby-Needs plasmon pole model (Godby & Needs, 1989a, 1989b). All many-body perturbation theory (MBPT) calculations were performed via Yambo package (Marini et al., 2009). In the one-shot calculations, Converged results attained by kinetic energy cut-offs of 80 Ry for screening dielectric function with 1800 bands. In the G0W0 approximation, G0 is built from kohn-sham orbitals, and QP energies are obtained as first order perturbation correction. QP energies were obtained by solving Dyson equation perturbatively as:

$$E_n^{QP} = E_{nk} + Z_{nk}\left(\Sigma(E_{nk}) - V_{nk}^{XC}\right) \qquad (1)$$

where E_{nk} is PBE-GGA KS energies, V_{nk}^{XC} is the exchange correlation potential, Σ is the expectation values of the self-energy, and Z_{nk} is the QP renormalization factor defined as (Shishkin & Kresse, 2007) :

$$1/Z_{nk} = 1 - \left[\frac{d\Sigma\,(\omega)}{d\omega}\right]_{\omega=E_{nk}} \qquad (2)$$

and the self-energy is spit into correlation part and screened-exchange (Shahrokhi & Leonard, 2017):

$$\Sigma = \Sigma_X + \Sigma_C \qquad (3)$$

3. Results and discussion

A. Structural properties

Firstly, in order to obtain an accurate result for electronic properties, a complete relaxation of the $CuSbS_2$ structure for both internal structure for anion and lattice parameters are conducted. The computed structural properties are mainly lattice constants. The optimised lattice constants of bulk phase and monolayer of CuSbS2 together with previous DFT calculations and experimental values are shown in Table 1. In the case of bulk phase of $CuSbS_2$ these tables show that largest portion of the error comes from lattice constant c which indicates that GGA-PBE xc functional cannot handle well the van der Waals (vdW) force. It has been established that PBE tends to underestimate the lattice constants . Interestingly, the values of lattice parameters calculated with inclusion of vdW interaction being a long range interaction force matched very well with experimental results (Takei, Maeda, & Wada, 2015). Furthermore, the distance between the Sb atoms of neighbouring atomic layers was found to be 2.02 Å and this value is reasonably in good agreement with experimental value of 2.05 Å (Ramasamy, Gupta, Palchoudhury, Ivanov, & Gupta, 2015).

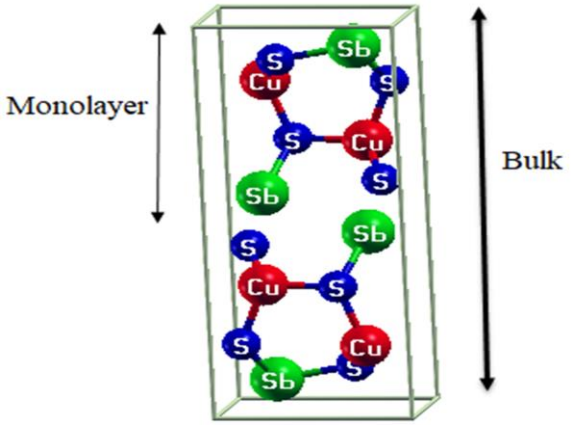

Figure 1: Optimized bulk crystal structure of $CuSbS_2$ unit cell

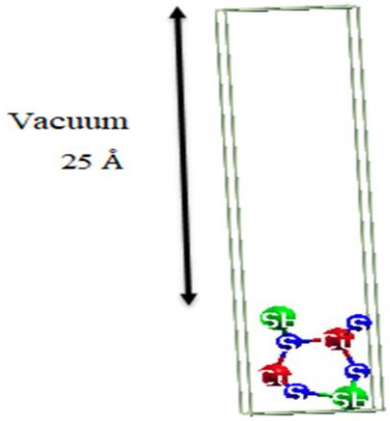

Figure 2 Optimized monolayer crystal structure of CuSbS2 unit cell

Table 1: Calculated lattice parameter of $CuSbS_2$

Method	Lattice Parameters for bulk phase		
	a(Å)	b(Å)	c(Å)
GGA-PBE	6.085	3.823	14.702
vdW-DF^{C09}x	6.019	3.785	14.438
Experiment (Takei et al., 2015)	6.020	3.791	14.485

B. Electronic Properties

By using the fully optimized structure of $CuSbS_2$, we have investigated the band structure of bulk and monolayer of $CuSbS_2$ material. The band structure calculations of bulk and monolayer of $CuSbS_2$ are computed my means of DFT within PBE and GW within GOWO approximation. The band structures were calculated along high-symmetry directions of the irreducible Brillouin zone (BZ) and Fermi energy level is set at 0 eV. The calculated energy band structure of bulk $CuSbS_2$ by means of GGA-PBE are displayed in Figure 3. For band structure calculation withing PBE, the energy separation between the valance band maximum and conduction band minimum was found to be 0.76 eV, this value is reasonably in agreement with previous DFT calculations (Alsaleh, Singh, & Schwingenschlögl, 2016; Maeda & Wada, 2015). However, this value is not consistent with available experimental data of 1.35-1.5 eV (Choi, Yeom, Ahn, & Seok, 2015; Welch et al., 2015; Yang et al., 2014; Zhou et al., 2009) and this effect is due to the approximations used in the exchange-correlation potential. Also, from the same figure, the conduction band minimum occurred at Γ point while the valance band maximum is located in between R and T, indicating that bulk $CuSbS_2$ has indirect bandgap. However, to correct this inconsistency in DFT calculation, we further performed G0W0 calculation. Conversely, G0W0 results bring the band gap value of bulk $CuSbS_2$ to 1.4 eV, this value is in good agreement with experimental results of 1.35-1.5 eV (Choi et al., 2015; Welch et al., 2015; Yang et al., 2014; Zhou et al., 2009). As the structures transfer from bulk to monolayer phase, the dimension considered reduce from three to two dimension (2D) as can be seen in Figure 2. Figure 5 and 6 show a graphs of band structures of CuSbS2 monolayer calculated with GGA-PBE and G0W0.

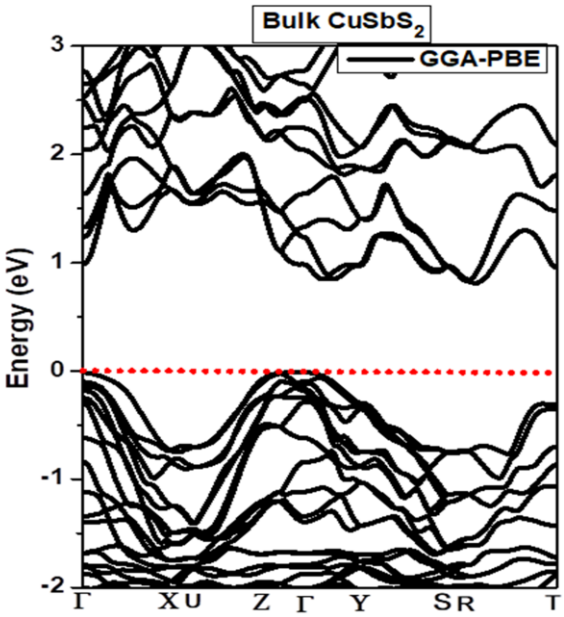

Figure 3 band structure of $CuSbS_2$ in bulk form for PBE method

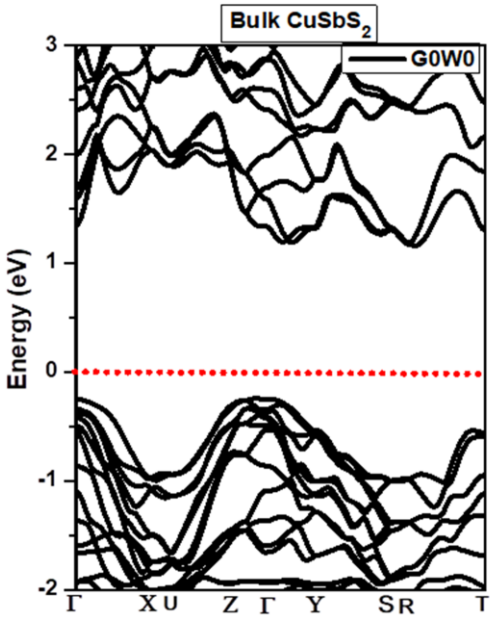

Figure 4 band structure of $CuSbS_2$ in bulk form for G0W0 method

In the case of $CuSbS_2$ monolayer, the energy separation between the valance band maximum and the conduction band minimum was found to be 0.35 eV with GGA-PBE and 0.64 eV by employing G0W0 method. The calculated band gap value of monolayer for both methods are smaller than that of the bulk form. This trend is consistent with previous studies (Alsaleh et al., 2016; Ramasamy et al., 2015; Ramasamy, Sims, Butler, & Gupta, 2014). Furthermore, the conduction band minimum and the valance band maximum occurred at Γ point,

indicating that $CuSbS_2$ monolayer has indirect bandgap. The nature of the band gap of $CuSbS_2$ monolayer agreed well with previous studies (Alsaleh et al., 2016; Ramasamy et al., 2015; Ramasamy et al., 2014). The reduction of band gap CuSbS2 monolayer is different from MoS2 in which the band gap increases by reducing the dimension to 2D (monolayer). The increase in band gap of MoS_2 monolayer is due to the presence of S atoms at the van der Waals gap whereas the positions of Mo atoms are the same in monolayer and bulk form. As a consequence, in the case of MoS_2 monolayer the S atoms dominated the valence band maximum is shifted to lower energy but not the Mo dominated the conduction band edge. Conversely, the positions of Sb and S atoms are located at the van der Waals gap in the case of $CuSbS_2$. Therefore, similar effect does not appear in the case of $CuSbS_2$ monolayer. The calculated bandgap values of $CuSbS_2$ for both bulk and monolayer together with experimental data are listed in Table 2.

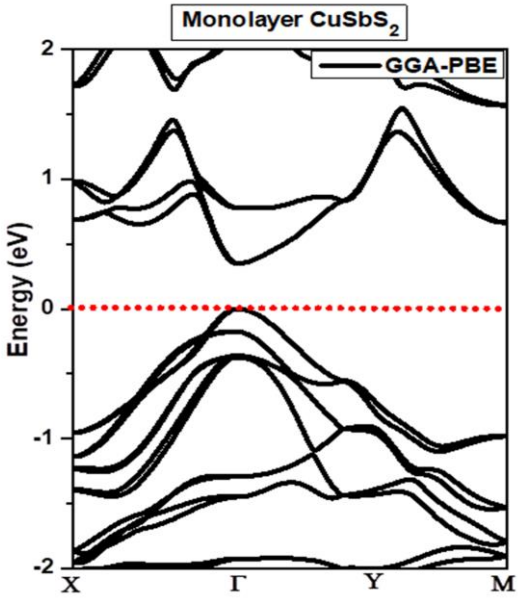

Figure 5 band structure of CuSbS2 monolayer for PBE method

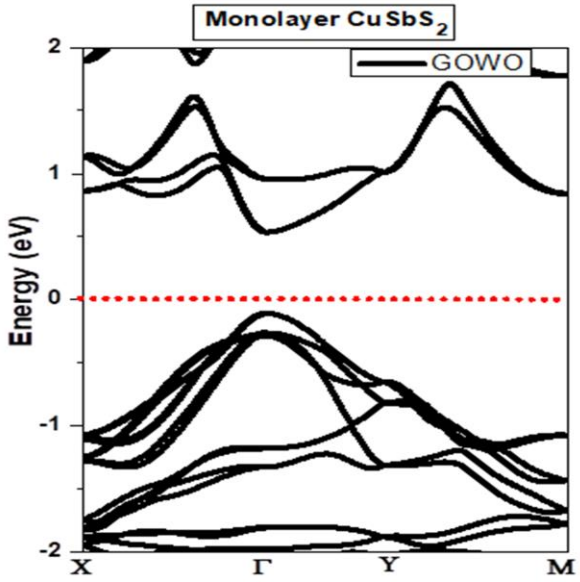

Figure 6 band structure of CuSbS2 monolayer for G0W0 method

Table 2 Calculated and experimental band gap value of $CuSbS_2$ in bulk form and monolayer

Method	Band gap value (eV)	
	Bulk	Monolayer
GGA-PBE	0.76	0.35
G0W0	1.40	0.64
PBE (Alsaleh et al., 2016)	0.74	0.15
TB-mBJ (Alsaleh et al., 2016)	1.02	0.21
TB-mBJ (Raju & Thangavel, 2020)	1.12	-
Exp. (Zhou et al., 2009)	1.35	-
Exp.(Yan et al., 2012; Yang et al., 2014)	1.40	-
Exp. (Choi et al., 2015; Welch et al., 2015)	1.5	-

4. Conclusions

In summary, we have presented the structural and electronic properties of $CuSbS_2$ in both bulk and monolayer. The structural parameters of CuSbS2 calculated with inclusion of van der Waals corrections are close to experimental results. The investigated electronic band structure reveals that CuSbS2 is indirect semiconductor material in the bulk form. We found the band gap value in this work to be 0.76 eV and 1.40 eV using GGA+PBE and G0W0 respectively. The band gap value of 1.4 eV is in good agreement with available experimental results of 1.35-1.5 eV (Choi et al., 2015; Welch et al., 2015; Yang et al., 2014; Zhou et al., 2009), after inclusion of GW quasiparticle self-energy correction. The band gap nature of $CuSbS_2$ switched from indirect to direct in the case of monolayer, because Sb atoms and S atoms are located at the van der Waals gap of the layered structure so that the valence band and conduction band edges are similarly affected by the transition into a 2D. In general, direct band gap nature and narrowing effect of CuSbS2 monolayer suggest that the investigated material is suitable for solar cells and optoelectronic applications.

References

Al Jibouri, R. H., & Buckley, S. (2020). Renewable Energy, a Clean Environment and Solar Desalination. In *Waste Management in MENA Regions* (pp. 377-401): Springer.

Alsaleh, N. M., Singh, N., & Schwingenschlögl, U. (2016). Role of interlayer coupling for the power factor of CuSbS 2 and CuSbSe 2. *Physical Review B, 94*(12), 125440.

Becquerel, E. (1839). On electric effects under the influence of solar radiation. *Compt. Rend., 9*, 561.

Chapin, D. M., Fuller, C., & Pearson, G. (1954). A new silicon p-n junction photocell for converting solar radiation into electrical power. *Journal of Applied Physics, 25*(5), 676-677.

Choi, Y. C., Yeom, E. J., Ahn, T. K., & Seok, S. I. (2015). CuSbS2-sensitized inorganic–organic heterojunction solar cells fabricated using a metal–thiourea complex solution. *Angewandte Chemie International Edition, 54*(13), 4005-4009.

Giannozzi, P., Baroni, S., Bonini, N., Calandra, M., Car, R., Cavazzoni, C., . . . Dabo, I. (2009). QUANTUM ESPRESSO: a modular and open-source software project for quantum simulations of materials. *Journal of physics: condensed matter, 21*(39), 395502.

Godby, R., & Needs, R. (1989a). Metal-insulator transition in Kohn-Sham theory and quasiparticle theory. *Physical review letters, 62*(10), 1169.

Godby, R., & Needs, R. (1989b). The metal-insulator transition in quasiparticle theory and Kohn-Sham theory. *Physical review letters, 62*(10), 1169-1172.

Javed, H. M. A., Que, W., Ahmad, M. R., Ali, K., Ahmad, M. I., ul Haq, A., & Sharma, S. (2020). Perspective of Nanomaterials in the Performance of Solar Cells. In *Solar Cells* (pp. 25-54): Springer.

LAWAL, A. (2017). Theoretical Study Of Structural, Electronic And Optical Properties Of Bismuth-Selenide, Bismuth-Telluride And Antimony-Telluride/Graphene Heterostructure For Broadband Photodetecto*R*. Universiti Teknologi Malaysia,

Lawal, A., Shaari, A., Ahmed, R., & Jarkoni, N. (2017a). First-principles investigations of electron-hole inclusion effects on optoelectronic properties of Bi2Te3, a topological insulator for broadband photodetector. *Physica B: Condensed Matter, 520*, 69-75.

Lawal, A., Shaari, A., Ahmed, R., & Jarkoni, N. (2017b). First-principles many-body comparative study of Bi2Se3 crystal: A promising candidate for broadband photodetector. *Physics Letters A, 381*(35), 2993-2999.

Lawal, A., Shaari, A., Ahmed, R., & Jarkoni, N. (2017c). Sb2Te3 crystal a potential absorber material for broadband photodetector: A first-principles study. *Results in physics, 7*, 2302-2310.

Lawal, A., Shaari, A., Ahmed, R., & Taura, L. (2018). Investigation of excitonic states effects on optoelectronic properties of Sb2Se3 crystal for broadband photo-detector by highly accurate first-principles approach. *Current Applied Physics, 18*(5), 567-575.

Lawal, A., Shaari, A., Ahmed, R., Taura, L., Madugu, L., & Idris, M. (2019). Sb2Te3/graphene heterostructure for broadband photodetector: A first-principles calculation at the level of Cooper's exchange functionals. *Optik, 177*, 83-92.

Maeda, T., & Wada, T. (2015). First-principles study of electronic structure of CuSbS2 and CuSbSe2 photovoltaic semiconductors. *Thin solid films, 582*, 401-407.

Marini, A., Hogan, C., Grüning, M., & Varsano, D. (2009). Yambo: an ab initio tool for excited state calculations. *Computer Physics Communications, 180*(8), 1392-1403.

Nagaoka, A., Takeuchi, M., Yoshino, K., Ikeda, S., Yasui, S., Taniyama, T., & Nishioka, K. (2019). Growth of CuSbS2 Single Crystal as an Environmentally Friendly Thermoelectric Material. *physica status solidi (a), 216*(15), 1800861.

Perdew, J. P., Burke, K., & Ernzerhof, M. (1996). Generalized gradient approximation made simple. *Physical review letters, 77*(18), 3865.

Pitchaiya, S., Natarajan, M., Santhanam, A., Asokan, V., Yuvapragasam, A., Ramakrishnan, V. M., . . . Velauthapillai, D. (2020). A review on the classification of organic/inorganic/carbonaceous hole transporting materials for perovskite solar cell application. *Arabian Journal of Chemistry, 13*(1), 2526-2557.

Raju, N. P., & Thangavel, R. (2020). Theoretical investigation of spin–orbit coupling on structural, electronic and optical properties for CuAB2 (A= Sb, Bi; B= S, Se) compounds using Tran–Blaha-modified Becke–Johnson method: A first-principles approach. *Journal of Alloys and Compounds*, 154621.

Ramasamy, K., Gupta, R. K., Palchoudhury, S., Ivanov, S., & Gupta, A. (2015). Layer-Structured Copper Antimony Chalcogenides (CuSbSe x S2–x): Stable Electrode Materials for Supercapacitors. *Chemistry of Materials, 27*(1), 379-386.

Ramasamy, K., Sims, H., Butler, W. H., & Gupta, A. (2014). Mono-, few-, and multiple layers of copper antimony sulfide (CuSbS2): a ternary layered sulfide. *Journal of the American Chemical Society, 136*(4), 1587-1598.

Shahrokhi, M., & Leonard, C. (2017). Tuning the band gap and optical spectra of silicon-doped graphene: Many-body effects and excitonic states. *Journal of alloys and compounds, 693*, 1185-1196.

Sharma, V., & Chandel, S. (2016). A novel study for determining early life degradation of multi-crystalline-silicon photovoltaic modules observed in western Himalayan Indian climatic conditions. *Solar Energy, 134*, 32-44.

Shishkin, M., & Kresse, G. (2007). Self-consistent G W calculations for semiconductors and insulators. *Physical Review B, 75*(23), 235102.

Sivagami, A., Biswas, K., & Sarma, A. (2018). Orthorhombic CuSbS2 nanobricks: Synthesis and its photo responsive behaviour. *Materials Science in Semiconductor Processing, 87*, 69-76.

Takei, K., Maeda, T., & Wada, T. (2015). Crystallographic and optical properties of CuSbS2 and CuSb (S1-xSex) 2 solid solution. *Thin solid films, 582*, 263-268.

Wan, L., Guo, X., Fang, Y., Mao, X., Guo, H., Xu, J., & Zhou, R. (2019). Spray pyrolysis deposited CuSbS 2 absorber layers for thin-film solar cells. *Journal of Materials Science: Materials in Electronics, 30*(24), 21485-21494.

Welch, A. W., Zawadzki, P. P., Lany, S., Wolden, C. A., & Zakutayev, A. (2015). Self-regulated growth and tunable properties of CuSbS2 solar absorbers. *Solar Energy Materials and Solar Cells, 132*, 499-506.

Yan, C., Su, Z., Gu, E., Cao, T., Yang, J., Liu, J., . . . Liu, Y. (2012). Solution-based synthesis of chalcostibite (CuSbS 2) nanobricks for solar energy conversion. *RSC Advances, 2*(28), 10481-10484.

Yang, B., Wang, L., Han, J., Zhou, Y., Song, H., Chen, S., . . . Tang, J. (2014). CuSbS2 as a promising earth-abundant photovoltaic absorber material: a combined theoretical and experimental study. *Chemistry of Materials, 26*(10), 3135-3143.

Zhou, J., Bian, G.-Q., Zhu, Q.-Y., Zhang, Y., Li, C.-Y., & Dai, J. (2009). Solvothermal crystal growth of CuSbQ2 (Q= S, Se) and the correlation between macroscopic morphology and microscopic structure. *Journal of Solid State Chemistry, 182*(2), 259-264.

Zou, X., Ji, L., Ge, J., Sadoway, D. R., Edward, T. Y., & Bard, A. J. (2019). Electrodeposition of crystalline silicon films from silicon dioxide for low-cost photovoltaic applications. *Nature communications, 10*(1), 1-7.